Contract No:

This document was prepared in conjunction with work accomplished under Contract No. DE-AC09-08SR22470 with the U.S. Department of Energy (DOE) Office of Environmental Management (EM).

Disclaimer:

Epithermal Neutron Resonance Analysis Using a Compact D-T Generator

E. Avram Klein and Areg Danagoulian

Department of Nuclear Science and Engineering
Massachusetts Institute of Technology
Cambridge, MA 02139

June 15, 2020

Abstract

Nuclear material identification and isotopic composition analysis are important capabilities for safeguards and the verification of nuclear arms control and nonproliferation treaties. Epithermal neutron resonance imaging has been proposed for spent fuel assay measurements, and the development of a mobile neutron imaging system could provide such a tool for on-site applications. This technique is highly sensitive to isotopes of interest for safeguards applications (e.g. ^{235,238}U, ^{238,239,240}Pu) and yields unique transmission spectra for a target containing actinides and some mid- and high-Z elements. Paired with a position-sensitive neutron detector, such a system could provide spatial information of the target isotopic composition. Recent progress in the development of high intensity neutron sources could make mobile epithermal neutron imaging designs increasingly feasible to serve as a tool for nuclear inspectors. In this work, Monte Carlo (MC) simulations were performed to further optimize a previous design for an epithermal neutron resonance-based analysis apparatus using a D-T portable neutron generator. Additionally, experimental work is being performed to test the feasibility of this method. The MC simulations of moderation time distributions for different moderator compositions and thicknesses were measured to provide a multi-group correction for neutron time-of-flight energy reconstruction.

Background

Since at least the 1980s, neutron resonance radiography has been explored as a means of imaging spent fuel for quality assurance – including crack and defect detection – and safeguards applications – such as detection of fuel rod diversion.[1, 2, 3, 4] The vast majority of these studies have been conducted at large-scale neutron beam-line facilities and, given the large, non-portable infrastructure required, are not suitable for mobile applications.[5] However, many nuclear safeguards applications require the ability to perform on-site analysis, in order to increase timeliness of analysis and limit the possibility of diverting nuclear material under inspection.[6] For this reason, the utility of neutron radiography can be significantly extended by the design of compact, possibly mobile, and relatively low-cost platforms. Improvements in portable neutron generators, such as pulsed deuterium-tritium (DT) fusion neutron sources, enable the production of a compact neutron beam with relatively high fluence at fixed energy.[7]

An isotope-specific technique that lends itself quite well for safeguards applications is neutron resonance transmission analysis (NRTA).[8, 9] NRTA uses the isotopic uniqueness of neutron resonances to differentiate neutron transmission ratios, thereby determining the isotopic and elemental composition of the target material. Due to the nature of these resonance interactions, a detector with limited solid angle will nearly only detect

the transmission of neutrons which have not interacted with the target material. Thus, the transmitted spectrum exhibits dips at energies that uniquely map to the resonance energies of the nuclei in the target material. The time between the neutron generation pulse and the time at which the neutron is measured at the detector provides the time-of-flight (TOF) of individual neutrons, enabling reconstruction of their energy.

$$E_n = \frac{1}{2} m_n \left(\frac{l_{TOF}}{t_{signal} - t_{pulse}} \right)^2 \tag{1}$$

In combination with known cross section data, the transmission spectrum can be used to precisely and simultaneously determine the areal density of the multiple isotopes that make up the target object. Many isotopes of interest to nuclear security (e.g. ^{235,238}U, ^{238,239,240}Pu) exhibit neutron resonances in the epithermal range (from 1 eV to 100 eV), while several common shielding materials do not (e.g. ^{1}H, ^{12}C, ^{16}O, ^{26}Fe, ^{82}Pb). By focusing on dips in the transmission spectra, the analysis is effectively transparent to the non-resonant organic and shielding materials and enables analysis and identification of fissile and fertile isotopes. By combining a well-collimated, portable neutron generator with carefully optimized moderation for epithermalization and shielding to prevent room-return, along with a pixelated detector to provide spatial resolution, isotopic imaging of nuclear materials can be achieved for mobile nuclear security applications.

Experimental Setup

A Geant4 application was developed to simulate the proposed neutron resonance spectroscopy apparatus. The apparatus consists of a shielded D-T neutron generator, a target object, an on-axis shielded neutron scintillation detector (^{6}Li-enriched GS20 glass), and an off-axis shielded gamma scintillation detector ($LaBr_3$ crystal).

The full experimental setup is shown in Figure 1.

Thickness of the ^{6}Li-enriched GS20 glass detector will also play a role in both number of detected epithermal neutrons and number of high-energy gammas detected. As thickness increases, a greater proportion of "true" epithermal neutrons will be detected, as well as higher energy neutrons incident within the desired TOF time window. In addition, gammas will deposit greater energy within the detector due to the increased thickness; this will reduce the gamma/neutron discrimination capability of the detector.

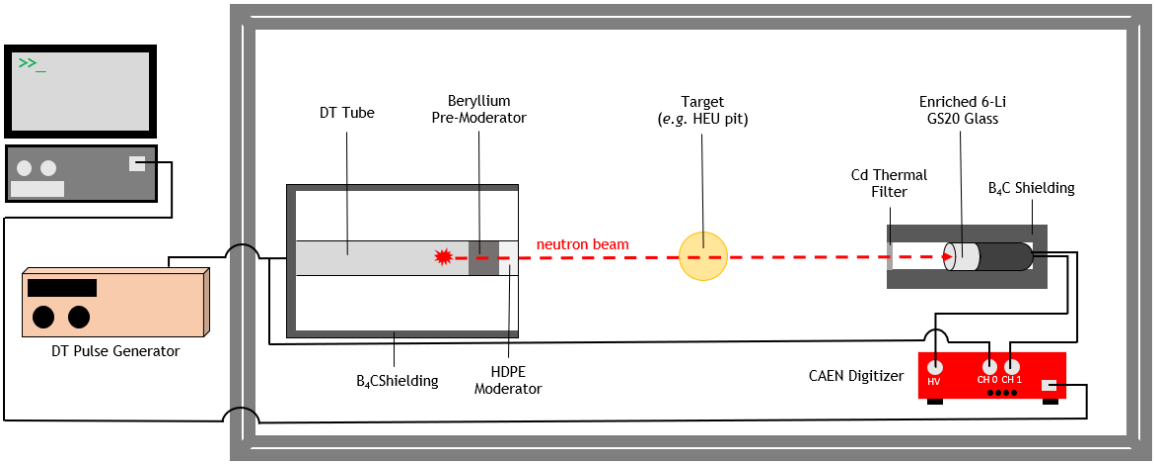

Figure 1: Diagram of the Experimental Setup. A D-T neutron generator is shielded by a box of borated polyethylene lined with boron carbide to prevent room return. The neutron beam is moderated in beryllium and then high-density polyethylene, incident on a target, and detected in a GS20 enriched ^{6}Li glass scintillator. Thermal neutrons are filtered by 5 mm of cadmium foil. All simulations in this paper were run for a $l_{TOF} = 1.50m$ unless otherwise noted.

Epithermal Neutron Production

D-T Neutron Generation

Development of a mobile apparatus for neutron resonance analysis depends on the production of an epithermal neutron beam of sufficient flux and time resolution to reconstruct neutron energy. In this paper, simulations of potential epithermal neutron beam generation assemblies were performed using Geant4.[10] All Geant4 simulations presented in this paper used the latest JEFF-3.3 evaluated neutron cross section data provided in Geant4-readable form by Mendoza, Cano-Ott et al.[11] High precision neutron scattering physics was turned on and thermal scattering neutron physics was implemented for hydrogenous material. Detector hits were output and post-processed using a custom Python analysis script.

The neutron output of the D-T neutron generator was calculated for a 90 keV accelerated deuteron beam on a tritium target and neutron yield for the t(d,n)α reaction was modeled using the DROSG-2000 code [12]. For a 90keV acceleration voltage, the neutron energy ranges from 14.72 MeV in the forward direction to 13.44 MeV in the backward direction. A uniform $5\mu s$ uncertainty time was added to each neutron's time-of-flight to model the finite pulse width of the DT generator. Rather than model the neutron production process which would be highly inefficient computationally, the neutron primary vertex was sampled uniformly over a 2.5 cm diamater disk, representing the tritium target. As a result, gamma production in the D-T reaction is not present in the Geant4 simulation. The angle of emission and corresponding neutron energy were randomly sampled based on the calculated neutron yield provided by the DROSG-2000 code.

The angular differential energy distribution was cut into 180 equally spaced slices in $\cos(\theta)$ space in the laboratory frame of reference. The distribution is slightly forward peaked in the laboratory reference frame. The differential neutron yield was used to produce a cumulative distribution function from which to sample neutron energy and angle of emission (θ_{lab}). A separate random number generator is used to sample for the azimuthal angle of neutron emission. In order to maximize computational efficiency, neutron production in the forward direction ($\theta_{lab} < 30^{\circ}$) is preferentially sampled. Because these neutrons are expected to compose only $\approx 15\%$ of all emitted neutrons, a weighting factor must be applied to any resulting neutron flux paramters.

Neutron Multiplication in ^{9}Be

The key disadvantages of using a D-T neutron generator for epithermal neutron production is the low epithermalization efficiency from $\sim$ 14 MeV to the epithermal (1-10 eV) range. In previous designs of the apparatus, moderators consisting solely of a variable thickness of high-density polyethylene (HDPE) were simulated.[13] Although a 10 cm thick HDPE moderator was previously shown to successfully moderate neutrons to the energy region of interest (1-10 eV), the epithermalization efficiency was low and distribution in neutron moderation time not insignificant, prompting consideration of alternative moderator assemblies.

In order to increase the epithermalization efficiency of the moderator assembly, a pre-moderator block of Beryllium was added before the moderator to soften the neutron output spectrum from the D-T generator. Beryllium has a moderate cross-section for the ^{9}Be(n,2n) reaction, with an energy threshold of $\approx 1.8MeV$. At 14 MeV, the (n,2n) cross-section is approximately one-third of the overall neutron cross section for Be, while the (n,γ) cross-section at MeV energies is $\sim$ 1E-6 b, [14] reducing the potential effects of a gamma background.

To test the effects of beryllium on the outgoing neutron spectrum and corresponding epithermalization efficiency, Geant4 simulations were initially conducted using hollow spheres of Beryllium and HDPE surrounding the front end of the deuteron acceleration tube containing the tritium target. The beryllium pre-moderator shell thickness was varied between 2.5 cm and 5.0 cm and the HDPE shell thickness was varied between 2.5 cm and 5.5 cm. These optimization studies found that epithermal neutron flux was maximized for a Be thickness of 5.0 cm and an HDPE thickness of 3.0 cm.

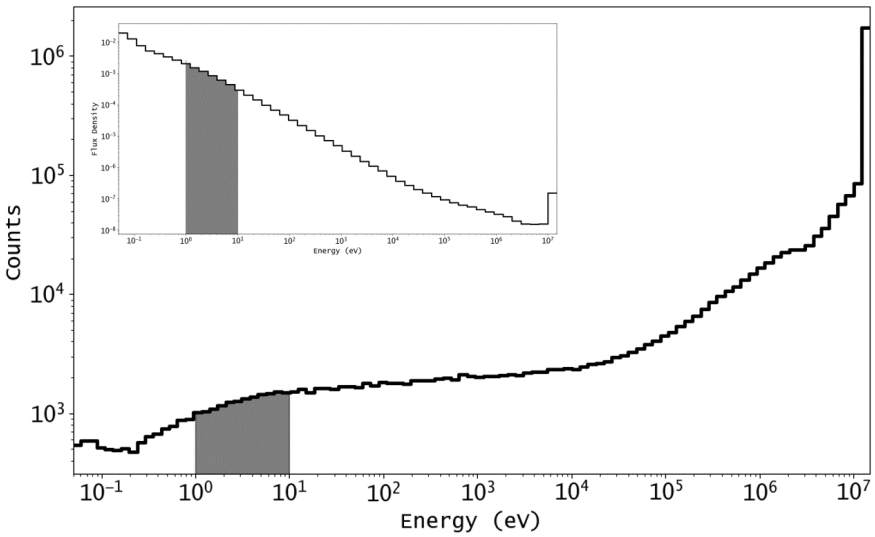

Figure 2: Neutron spectrum at front surface of moderator assembly, which consists of a 5 cm Be pre-moderator and 3 cm HDPE moderator. Neutron flux density is shown in the inset. Neutrons between 1 and 10 eV are shown in the dark gray region in both plots.

Because the outer HDPE shell does produce 2.23 MeV γ rays through the (n,γ) reaction on ^{1}H – that may be indistinguishable from neutrons in detection by the glass scintillator – efforts were made to reduce the HDPE thickness. In order to minimize the number of gammas produced, the production of 2.2 MeV gammas was analyzed as the thickness of the HDPE outer shell was varied. Initial results demonstrate that the HDPE thickness could be reduced from 4.0 cm to 3.0 cm without significant change in epithermal neutron production, while reducing the number of gammas above 0.5 MeV by $\approx 30\%$. For a 3.0 cm thick outer shell, the ratio of > 1 MeV gammas to epithermal neutrons (with corresponding epithermal TOF-reconstructed energies) was approximately 1:2.

The optimized moderator assembly of sequential shells was then compared with the previous experimental setup which included borated polyethylene shielding with a boron carbide (B_4C) lining. The additional shielding demonstrated increased epithermal neutron flux and so the previous assembly was modified by replacing the 10 cm of HDPE with 5cm of Be and 3 cm of HDPE. This configuration is used for all simulations presented in the rest of this paper. The simulated neutron spectrum in the forward direction at the surface of the new moderator assembly is shown in Figure 2, comparable in flux density profile to that given in previous experimental studies.[15]

The time spread in neutron moderation for the new assembly, as a function of energy, is presented in Figure 3. As is the case for an HDPE-only moderator, Δt_{mod} increases for decreasing energy, and is submicrosecond for neutron energies above 1 eV. The moderation time can be accounted for by applying an energy group correction, subtracting the median neutron moderation time from the total time-of-flight. Given that all commercially available, portable DT neutron generators have minimum pulse widths in the range of 3-5 μs [7], the moderation time spread is not a limiting factor for the proposed setup.

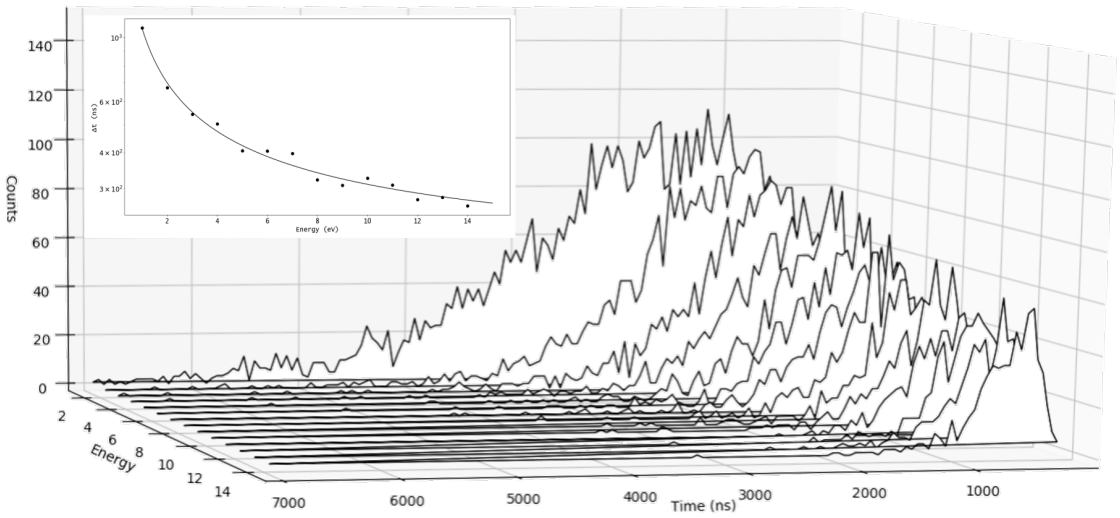

Figure 3: Neutron spectrum at front surface of moderator assembly, which consists of a 5.0 cm Be pre-moderator and 3.0 cm HDPE moderator. The insert shows the interquartile range in moderation time for the resultant neutron energy region 1-15 eV.

Epithermal Neutron Detection

The previous apparatus design used a 1" thick ^{6}Li glass scintillator for neutron detection via the $^6\mathrm{Li}(n,\alpha)t$ reaction which deposits 4.78 MeV within the detector. Gamma particles incident on the detector and correlated with neutron generation are easily rejected by detection time windowing and a suitable pulse height cut. However, initial experimental studies using a 1" thick ^{6}Li glass scintillator indicated that while this thickness had terrific neutron detection efficiency, it showed poor γ/n discrimination. Subsequent Geant4 simulations of a 1.0 cm thick and 5 mm thick scintillator demonstrated corresponding $\sim 75\%$ and $\sim 50\%$ neutron detection efficiencies with great n/γ discrimination (Figure 4.) Furthermore, the thinner neutron detector mitigated inelastic scattering of $\sim$ 14 MeV neutrons incident on the detector from the D-T neutron generator, further reducing background on the neutron transmission spectrum.

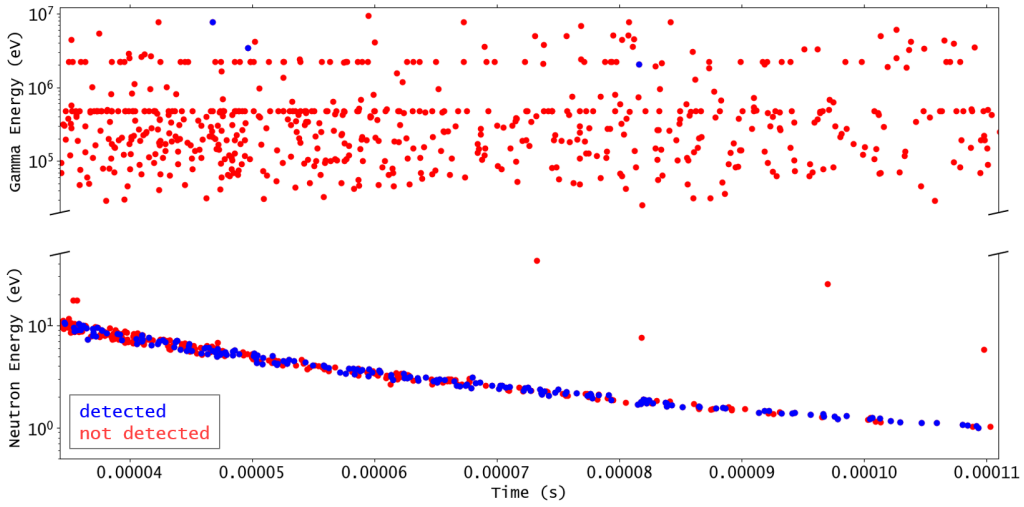

Figure 4: Geant4 simulation of neutrons and gammas incident on the detector plotted with their true energy as a function of corrected time-of-flight. The detection threshold was assumed to be 4 MeV deposited for neutrons and 1 MeV deposited for gammas. Note the discontinuity in scale between neutron and gamma energies.

Results

TOF Energy Reconstruction

To determine the open beam neutron spectrum at the detector, 1.5E8 importance-sampled events were run in a Geant4 simulation using the experimental setup detailed in the previous sections. Figure 5 displays the comparison of the TOF-reconstructed detector hits ("actual"), which includes both neutrons and gammas, compared to the true epithermal neutron hits ("ideal" or "true"). Times-of-flight were corrected by centering them on an assumed $4\mu s$ pulse width. The detection threshold was assumed to be 4 MeV deposited for neutrons and 1 MeV deposited for gammas. Despite some differences in the histogram binning, the kernel density estimation (KDE) of the actual spectrum matches very well that of the true spectrum.

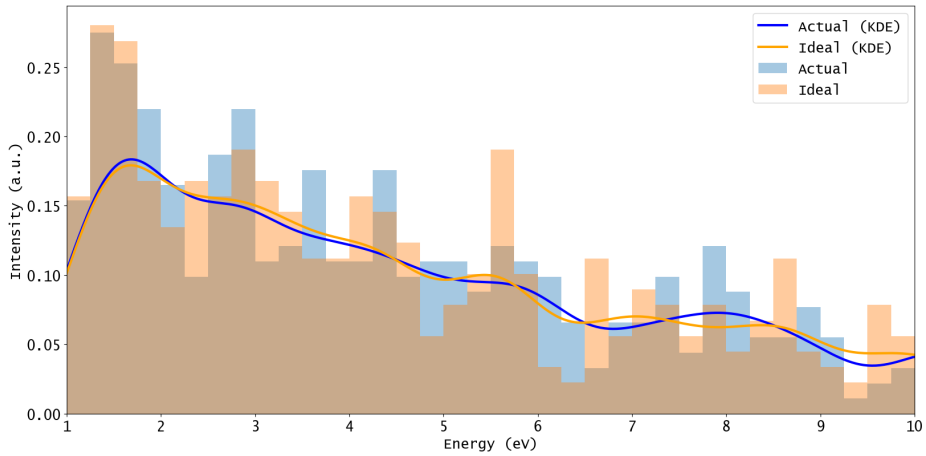

Figure 5: Kernel density estimation (KDE) and histograms of the detected neutron flux at the detector. The actual flux is a plot of the reconstructed energy of all particles (*i.e.* neutrons and gammas) detected within the epithermal TOF window, whereas the ideal flux plots the true energy of detected neutrons.

Assuming a 10% duty cycle, the epithermal neutron flux at the detector was 0.367 $n/cm^2/s$ and the epithermal neutron detection efficiency was 42.4%. This is a factor of 4 improvement over the previously simulated HDPE-only moderator assembly. The TOF-reconstructed energy of 95% of epithermal neutrons were within 15% of their true energies, and the median error in TOF-reconstructed energy was 0.21 eV, within the range of many epithermal neutron resonance widths of interest. Neutron room return has effectively been eliminated by the boron carbide shielding on neutron generator and detector and the 5 mm of cadmium foil placed along axis. High-energy (>1 MeV) gammas did appear during the epithermal neutron TOF window, but most deposited little to no energy and should be easily rejected with pulse height analysis.

Isotopic Analysis of HEU Pit

As a first test of the feasibility, an HEU pit based on Fetter et al.'s description [16] was constructed in Geant4 and placed in the path of the neutron beam. 3.0E+8 neutron events were simulated with a forward bias and the post-processing to simulate detector digitization was conducted. The TOF-reconstructed transmitted epithermal neutron spectrum was compared to that of the open beam spectrum. Histograms of TOF-reconstructed neutron energy bins and corresponding KDEs are plotted in Figure 6, with expected transmission based on ENDF evaluated cross section data provided below the figure. These spectra represent a 15 minute open beam run (assuming a 10% duty cycle) and a 5 minute target run. Because of the low efficiency in epithermal neutron,

transmission, and detection, variance reduction techniques in Geant4 are being employed to reduce CPU time required for longer scans.

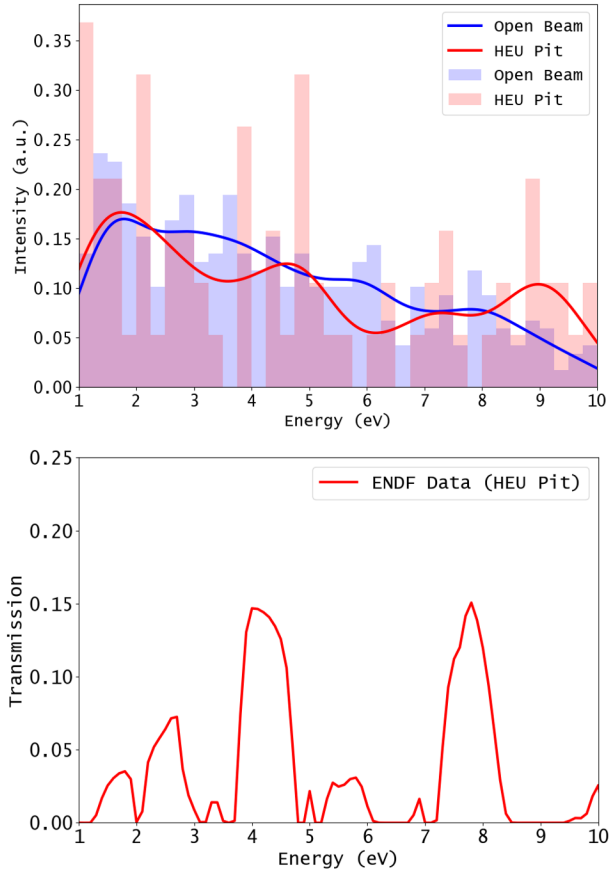

Figure 6: Kernel density estimation (KDE) and histograms for a 15 minute simulated open beam scan and a 5 minute simulated scan of a mock HEU pit (93.5% ^{235}U. Note the offset in the resonant attenuation dips likely due to nonlinear effects in the correction and conversion of time-of-flight to neutron energy.

Resonant attenuation dips can be seen in the regions 3-4 eV and 5-7 eV corresponding to ^{235}U and a combination of ^{234}U, ^{235}U, and ^{238}U resonances, respectively. At higher energies, the open beam neutron flux decreases to the point that transmission cannot be obtained with sufficient accuracy. The resonances appear to be shifted in the simulated data compared to calculation and is likely due to nonlinear effects in the correction and conversion of time-of-flight to neutron energy. Future work will aim to perform all KDE and other post-processing operations in the time domain to eliminate these effects.

Conclusion

Epithermal neutron resonance analysis is a proven technique for imaging mid- and high-Z materials, for which X-Ray and other passive imaging techniques are insufficient. The extension of this technique to a more compact apparatus would expand the application space and potentially provide a new tool for international nuclear inspectors and nuclear authorities around the world. Incremental improvements to previous designs demonstrate greater neutron flux, enhanced neutron/gamma discrimination, and reduced moderation time spread. Initial tests of neutron energy reconstruction via time-of-flight and isotopic analysis of a mock HEU pit show promise for successful application to nuclear nonproliferation and international safeguards applications.

Acknowledgements

This research was performed under appointment to the Nuclear Nonproliferation International Safeguards Fellowship Program sponsored by the National Nuclear Security Administration's Office of International Nuclear Safeguards (NA-241).

References

[1] James W Behrens, Ronald G Johnson, and Roald A Schrack. Neutron resonance transmission analysis of reactor fuel samples. *Nuclear technology*, 67(1):162–168, 1984.

[2] A.S. Tremsin, S.C. Vogel, M. Mocko, M.A.M. Bourke, V. Yuan, R.O. Nelson, D.W. Brown, and W.B. Feller. Non-destructive studies of fuel pellets by neutron resonance absorption radiography and thermal neutron radiography. *Journal of Nuclear Materials*, 440(1-3):633–646, 9 2013.

[3] Aaron E. Craft, Daniel M. Wachs, Maria A. Okuniewski, David L. Chichester, Walter J. Williams, Glen C. Papaioannou, and Andrew T. Smolinski. Neutron Radiography of Irradiated Nuclear Fuel at Idaho National Laboratory. *Physics Procedia*, 69:483–490, 1 2015.

[4] Sven C. Vogel, Darrin David Byler, Erofili Kardoulaki, Adrian Simon Losko, Kenneth James Mcclellan, Anton Tremsin, Anders David Ragnar Andersson, and Joshua Taylor White. Neutron Resonance Spectroscopy Applications for Nuclear Fuel Characterization. Technical report, Los Alamos National Laboratory, 2018.

[5] *Neutron Radiography: Proceedings of the First World Conference*.

[6] International Atomic Energy Agency Department of Safeguards. Research and Development Plan: Enhancing Capabilities for Nuclear Verification. Technical Report STR-385, International Atomic Energy Agency, Vienna, Austria, 2018.

[7] Calvin Elroy Moss, William L. Myers, Gary M. Sundby, David L Chichester, and James P Johnson. Survey of Neutron Generators for Active Interrogation. Technical report, Los Alamos National Laboratory, 2017.

[8] J W Sterbentz and D L Chichester. Neutron Resonance Transmission Analysis (NRTA): A Nondestructive Assay Technique for the Next Generation Safeguards Initiative's Plutonium Assay Challenge. Technical report, Idaho National Laboratory, 2010.

[9] P. Schillebeeckx, B. Becker, H. Harada, and S. Kopecky. Neutron resonance spectroscopy for the characterization of materials and objects. pages 10–66. Springer, Berlin, Heidelberg, 2015.

[10] S Agostinelli et al. Geant4—a simulation toolkit. *Nuclear Instruments and Methods in Physics Research Section A: Accelerators, Spectrometers, Detectors and Associated Equipment*, 506(3):250–303, 2003.

[11] Emilio Mendoza and Daniel Cano-Ott. Evaluated neutron cross section libraries for the Geant4 code, 2018.

[12] M. Drosg. DROSG-2000: Neutron Source Reactions, 2017.

[13] Ezra M Engel, Ethan A Klein, and Areg Danagoulian. Feasibility study of a compact neutron resonance transmission analysis instrument. *AIP Advances*, 10(1):15051, 2020.

[14] National Nuclear Data Center. Sigma - Evaluated Nuclear Data File (ENDF) Retrieval & Plotting.

[15] J Jordanova and O Penchev. Neutron leakage spectra through a beryllium slab bombarded by 14 MeV neutrons. *Annals of Nuclear Energy*, 20(10):653–658, 1993.

[16] Steve Fetter, Valery A. Frolov, Marvin Miller, Robert Mozley, Olea F. Prilutskv, Stanislav N. Rodionov, and Roald Z. Sagdeev. Detecting Nuclear Warheads. *Science & Global Security*, 1(3-4):225–253, 1990.